

Crystallization Behavior of Fully Biodegradable Poly(Lactic Acid)/Poly(Butylene Adipate-co-Terephthalate) Blends

Hanwen Xiao,¹ Wei Lu,¹ Jen-Taut Yeh^{1,2,3}

¹Ministry of Education, Key Laboratory for the Green, Preparation and Application of Functional Materials, Institute of Composite Materials, Faculty of Materials Science and Engineering, Hubei University, Wuhan 430062, China

²Key Laboratory of Green Processing and Functional Textiles of New Textile Materials (Wuhan University of Science and Engineering), Ministry of Education, Wuhan, China

³Department and Graduate School of Polymer Engineering, National Taiwan University of Science and Technology, Taipei, Taiwan

Received 9 June 2008; accepted 25 November 2008

DOI 10.1002/app.29800

Published online 12 March 2009 in Wiley InterScience (www.interscience.wiley.com).

ABSTRACT: Both poly(lactic acid) (PLA) and poly(butylene adipate-co-terephthalate) (PBAT) are fully biodegradable polyesters. The disadvantages of poor mechanical properties of PLA limit its wide application. Fully biodegradable polymer blends were prepared by blending PLA with PBAT. Crystallization behavior of neat and blended PLA was investigated by differential scanning calorimetry (DSC), polarizing optical microscopy (POM), and wide angle X-ray diffraction (WAXD). Experiment results indicated that in comparison with neat PLA, the degree of crystallinity of PLA in various blends all markedly was increased, and the crystallization mechanism almost did not change. The equilibrium melting point of PLA

initially decreased with the increase of PBAT content and then increased when PBAT content in the blends was 60 wt % compared to neat PLA. In the case of the isothermal crystallization of neat PLA and its blends at the temperature range of 123–142°C, neat PLA and its blends exhibited bell shape curves for the growth rates, and the maximum crystallization rate of neat PLA and its blends all depended on crystallization temperature and their component. © 2009 Wiley Periodicals, Inc. *J Appl Polym Sci* 112: 3754–3763, 2009

Key words: biodegradable polymer; crystallization; equilibrium melting point; blends

INTRODUCTION

Biodegradable polymers have received much more attention in the last two decades because of their potential applications in the fields related to environmental protection and the maintenance. PLA is biodegradable crystalline polyester, which can be produced from renewable sources. The crystal structure and crystallization behavior of PLA have been investigated extensively.^{1–3} Hard and brittle mechanical properties of PLA limit its development and practical application; therefore, several modifications have been proposed to improve processing and mechanical properties, such as copolymerization, plasticization, and polymer blending. Among the several modifications, polymer blending is regarded as a useful and economical way to produce new materials with a wide range of properties. Blends of PLA with other polymers, such as poly(ethylene succinate) (PES),⁴ natural poly(3-hydroxybutyrate)

(PHB),⁵ synthetic atactic poly(3-hydroxybutyrate) (a-PHB),⁶ poly(methyl methacrylate) (PMMA),⁷ poly(vinyl phenol) (PVPh),⁸ poly(vinyl acetate) (PVAc),⁹ poly(*p*-dioxanone),¹⁰ poly(3-hydroxybutyrate-co-3-hydroxyvalerate) (PHBV),¹¹ poly(vinyl alcohol) (PVA),¹² poly(butadiene-co-acrylonitrile) (NBR),¹³ and poly(butylene adipate-co-terephthalate) (PBAT),¹⁴ have been studied to modify the properties and expand its practical application.

PLA was reported to be immiscible with PBAT,¹⁴ the addition of glycidyl methacrylate (GMA) was found to enhance the interfacial adhesion between PLA and PBAT, the tensile toughness of the PLA/PBAT blends was greatly increased without severe loss in tensile strength when 2 or 5 wt % GMA was added to PLA/PBAT blends and the impact strength of the blends was also significantly improved at 1 wt % of GMA addition.¹⁵ How to improve the miscibility between PLA and PBAT has been carrying out in our group and the detail result will be reported in a separate article.

PBAT is synthetic biodegradable aromatic polyester with good mechanical properties, especially its elongation at break, its crystal structure, morphology and melting behavior have been reported in literature.^{16,17} The addition of PBAT was found to accelerate the crystallization rate of PLA but had little

Correspondence to: J.-T. Yeh (jyeh@tx.ntust.edu.tw).

Contract grant sponsor: Ministry of Education Key Laboratory for the Green Preparation and Application of Functional Materials.

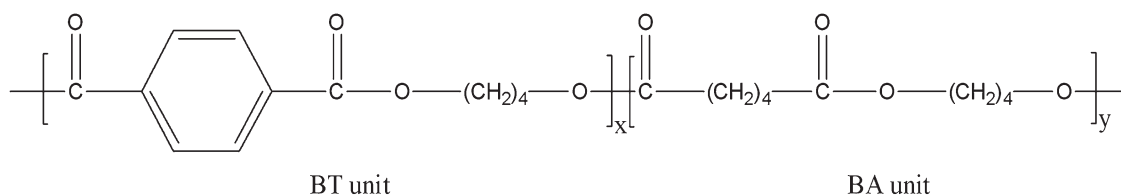


Figure 1 Chemical structure of poly(butylene adipate-co-terephthalate).

effect on its final degree of crystallinity.¹⁴ The PLA crystallization rate, both the melt or the glassy state, was enhanced by the presence of poly(ϵ -caprolactone) (PCL) domains.¹⁸ Qiu et al. studied the crystallization of PLA/PES blends by DSC and found that the crystallization rate of PLA was accelerated with the increase of PES in the blends while the crystallization mechanism did not change.⁴ Till now, less work has been performed on the crystallization behavior of PLA/PBAT blends. The features of PLA/PBAT blends can be summarized as follows. First, PLA/PBAT blends are fully biodegradable polymer blends, because both the components are biodegradable polyester. Second, PLA/PBAT blends are crystalline/semicrystalline polymer blends and thus can provide different phase behavior depending on blend composition. Third, crystallization rate of PLA can be modulated in the blends by changing the blend composition and crystallization condition and the physical properties of a crystalline polymer depend strongly on its crystal structure and the degree of crystallinity. Therefore, it is believed that the crystallization behavior study of this work will be helpful for a better understanding of the relationship between structure and properties of biodegradable polymer blends. It should be of great interest and importance to modify the properties and expand the practical application for PLA from both academic and industrial viewpoints.

EXPERIMENTAL

Materials

The commercial PLA (Natureworks PLA 4032D) exhibits a density of 1.25 g/cm³, a weight-average molecular weight of 207 kDa, polydispersity of 1.74 (GPC analysis), and a glass transition temperature and melting point of 60 and 168°C (differential scanning calorimeter (DSC) analysis), respectively. The PBAT (Ecoflex FBX 7011, BASF Corp.) with density of 1.26 g/cm³ exhibits a weight-average molecular weight of 145 kDa, polydispersity of 2.40 (GPC analysis), and a glass transition temperature and melting point of -30 and 122°C (DSC analysis), respectively. Both polymers are supplied in granular form and used as received, their chemical structure are shown in Figures 1 and 2.

Blends preparation

The neat PLA and PBAT granules are predried in vacuum oven at 70°C for 24 h before use. The dried granules of PLA and PBAT are mixed together with different weight ratios of 100/0, 80/20, 60/40, 40/60, and 0/100 in Haake internal mixer (Rheomex 600P, Germany) with Roller-Rotors R600 for 3 min. The mixing rollers are maintained at 90 rpm and the temperature was set at 185°C. Thenafter the melts are compressed to films with a thickness of around 0.5 mm for 3 min at 190, 150, and 185°C and 10 MPa for PLA, PBAT and their blends, respectively.

Thermal analysis

The thermal characteristics of the blends are determined using a differential scanning calorimeter (DSC Q100, TA instrument, USA) in nitrogen atmosphere (circulation). Samples (about 10 mg) are cut from a sample and placed in sealed aluminum pans. For each sample, the following thermal cycles is applied: a first scan is made from room temperature to 185°C for 3 min to destroy any thermal history. Then the sample is cooled to -50°C rapidly. The actual measurement is performed during a second heating from -50 to 200°C at a heating rate of 10°C/min. A nitrogen flow is maintained throughout the test. The glass transition temperature (T_g), cold crystallization temperature (T_{cc}), melting temperature (T_{m1} and T_{m2}), the degree of crystalline (x_c) and are determined in the second heating scan. On the basis of the heat of fusion of 100% crystallinity of PLA (93 J/g),¹⁹ the degree of crystallinity of PLA and its blends is calculated from the melting endotherms of the samples and normalized with respect to the composition of each component in the blends.

The equilibrium melting temperature (T_m^0) of PLA and its blends are determined by extrapolation to

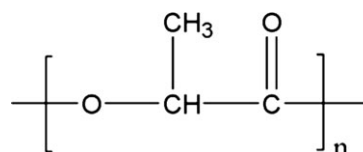


Figure 2 Chemical structure of poly(lactic acid).

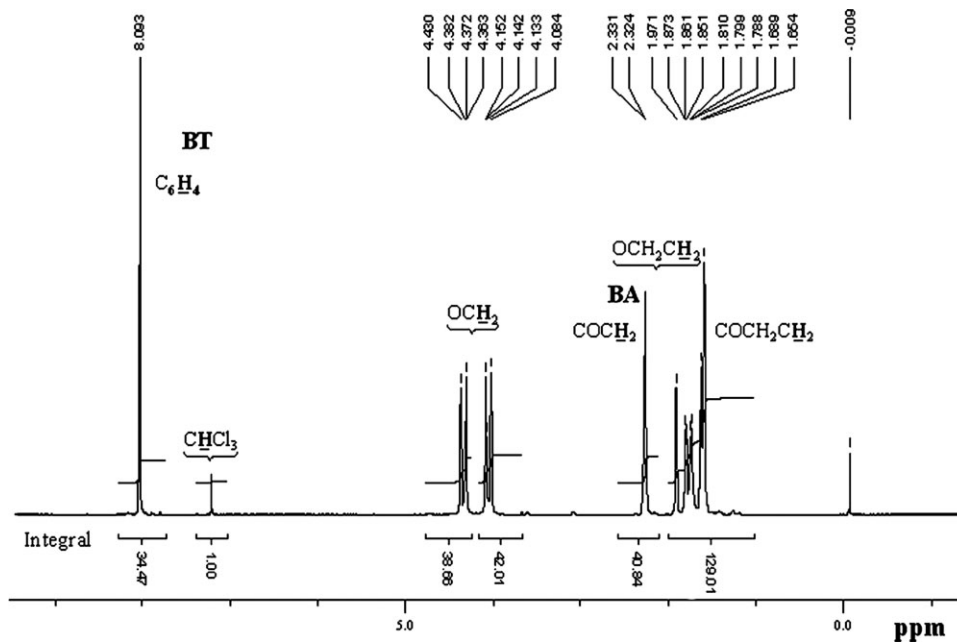


Figure 3 $^1\text{H-NMR}$ spectrum of PBAT.

the lines of $T_m = T_c$ according to the Hoffman-Weeks equation.²⁰ PLA and its blends are heated to 185°C and maintaining for 3 min and then cooled and crystallized at different temperature (120, 125, 130, 135, and 140°C, respectively). At each temperature, annealing lasts for 10 h in nitrogen atmosphere, and then the samples were cooled to 50°C at 40°C/min and heated to 200°C at 10°C/min for determining the melting points.

The isothermal crystallization from the melt is also examined by DSC. The samples are cooled to 128°C at a cooling rate of 50°C/min to crystallize PLA and its blends for 2 h after being held at 185°C for 3 min to destroy any thermal history.

Polarized optical microscopy

A polarized optical microscope (Olympus BX51) equipped with a Linklam THMSE 600 hot stage is used to investigate the spherulitic morphology and growth of PLA and its blends. The samples are first placed between glass slides and molten on a hot stage at 185°C for 3 min and then rapidly cooled to given crystallization temperature. Annealing lasts for given time periods.

Wide-angle X-ray diffraction

X-ray diffraction is used to probe the crystallinity of neat PLA, PBAT and their blends. Thin film samples are analyzed using a wide-angle X-ray diffraction apparatus (shimadu XRD-6000) by Cu $K\alpha$ ($\lambda = 0.154$ nm) under a voltage of 35 KV and a current of 25 mA radiation. Diffraction intensities are counted at

0.02° -steps and the scanning speed is 5°/min. The spectra are recorded in an angular range $5^\circ < 2\theta < 40^\circ$ at room temperature.

Nuclear magnetic resonance spectroscopy

$^1\text{H-NMR}$ spectra are recorded using a Bruker AS 600 high resolution $^1\text{H-NMR}$ spectrophotometer. Figure 3 shows the $^1\text{H-NMR}$ spectrum of PBAT, dissolved in CDCl_3 . The ratio between each monomer unit has been determined by $^1\text{H-NMR}$. The integration of the peaks of the adipate unit (BA) and the terephthalate unit (BT), respectively, at 2.33 and 8.09 ppm, gives PBAT composition: 54.5% of BA and 45.5% of BT.

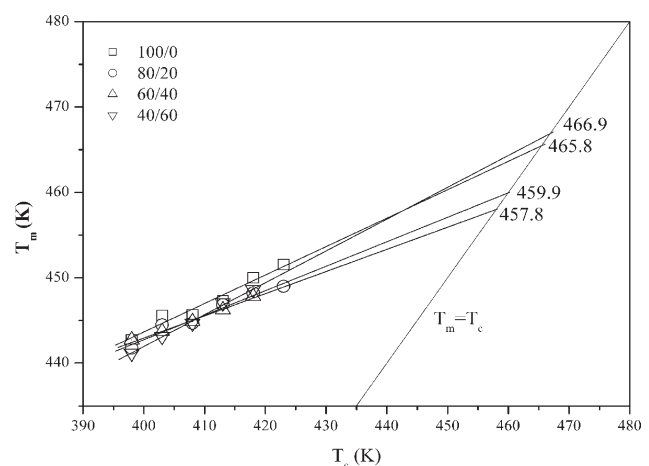


Figure 4 Hoffman-Weeks plot for neat PLA and its blends.

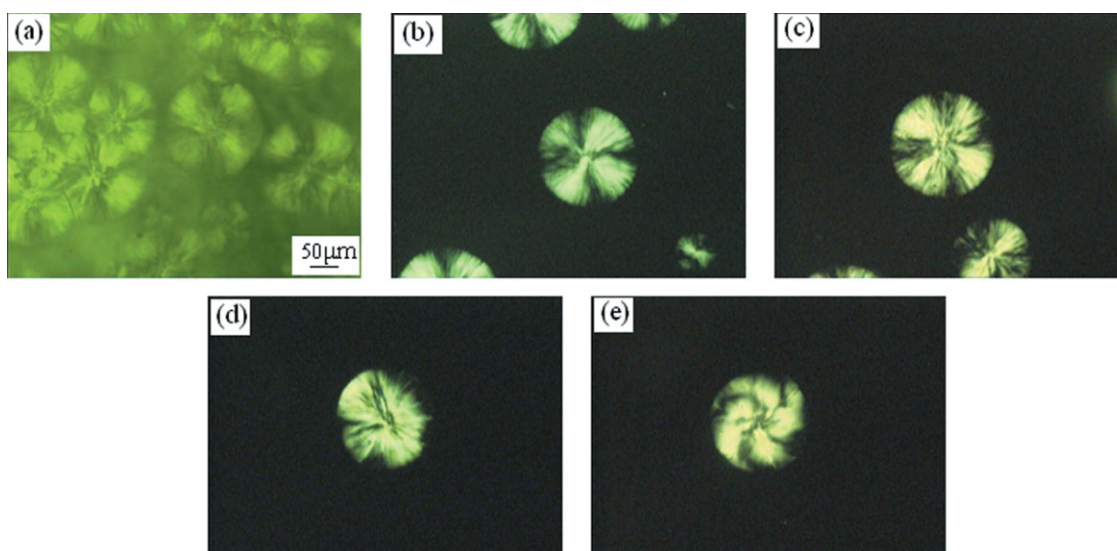


Figure 5 Polarizing optical micrographs of PLA crystallized isothermally for 12 min. (a) 123°C; (b) 128°C; (c) 132°C; (d) 137°C, and (e) 142°C. [Color figure can be viewed in the online issue, which is available at www.interscience.wiley.com.]

RESULTS AND DISCUSSION

Equilibrium melting point

Figure 4 shows the Hoffman-Weeks plots of neat and blended PLA with PBAT at various compositions. The equilibrium melting point (T_m^0) is obtained from the intersection of this line with the $T_m = T_c$ equation. T_m^0 for neat PLA is about 192.8°C, which is lower than previously reported values in the range from 207 to 212°C.²¹ In the blends, the equilibrium melting point decreases largely in the early stage, but this depression is decreased with increasing PBAT content. The maximum extent of this melting point depression is about 8°C in the blend with 40 wt % PBAT, where T_m^0 is 184.8°C. It is worth noting that in contrast to blends containing 20 and 40 wt % PBAT, the equilibrium melting point of PLA in the blend containing 60 wt % PBAT increases, even is higher than that of neat PLA, and indicating that the crystalline phase in the blend containing 60 wt % PBAT is more perfect than those of neat PLA and two blends mentioned above. The overall effect of the addition of an immiscible PBAT on spherulite growth rate of a crystallizable PLA depends on the values of the energy barriers that need to be overcome to reject and/or deform the noncrystallizable PBAT. It may be that PBAT produces a decrease in spherulitic growth rate of PLA in the PBAT-rich blends, which was also measured in blends of iPP with PDCHI, POM with P3HB, iPP with EPR.^{22–25} The lowering of spherulitic growth rate indicates higher nucleation density of crystal nuclei compared to neat PLA and two other blends with 20 and 40 wt % PBAT and favors the formation of perfect crystalline phase.

Spherulitic morphology

Figures 5 and 6 shows that neat and blended PLA with 20 wt % PBAT crystallized in the range of 123–142°C and it shows the spherulites formed after isothermal crystallization at the indicated temperatures. It is observed that spherulites display typical Maltese Cross at the temperature range of 123–132°C, but the typical Maltese Cross disappears at crystallization temperatures of 137°C or more. Moreover, the brightness of polarized light in the edge of spherulites significantly decreased. The spherulitic morphology of PLA in the blends displays marked change when PBAT content is 40 and 60 wt % as shown in Figures 7 and 8. The spherulites do not display typical Maltese Cross and have impinged into each other in 12 min at lower than 132°C when PBAT content in the blends is 40 wt %. It becomes more apparent that Maltese Crosses disappear completely and spherulites are badly distorted at lower than 123°C when PBAT content in the blends is 60 wt %. In particular, the spherulites do not fill the volume completely.

Spherulitic growth rate

The spherulitic growth rates of neat and blended PLA are measured by following the development of radius with time. PLA spherulites show a linear growth until their impingement during the crystallization process. Figure 9 shows the temperature and component dependence of the spherulitic growth rates of neat and blended PLA at different crystallization temperature. Neat and blended PLA with 20 and 40 wt % PBAT exhibit a bell shape curve for the growth rates in the crystallization temperature range

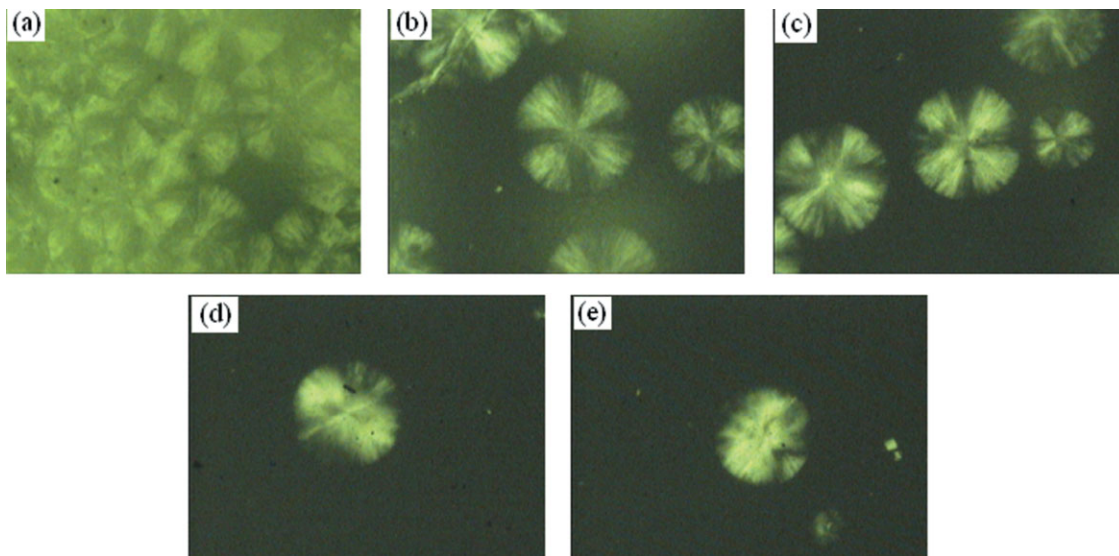


Figure 6 Polarizing optical micrographs of PLA/PBAT (weight ratio: 80/20) crystallized isothermally for 12 min. (a) 123°C; (b) 128°C; (c) 132°C; (d) 137°C, and (e) 142°C. [Color figure can be viewed in the online issue, which is available at www.interscience.wiley.com.]

of 123–142°C. From Figure 9, it can be seen that the crystallization rate of neat and blended PLA with 20 wt % PBAT increases with increasing crystallization temperature until 132°C, shows a maximum value of 0.282 and 0.31 $\mu\text{m/s}$ for the growth rate at 132°C. Above 132°C, neat PLA crystallization rate decreases. Crystallization growth rate of blended PLA with 40 wt % PBAT has a maximum value of 0.32 $\mu\text{m/s}$ at 128°C as shown in Figure 9. Below 140°C, the crystallization growth rates of PLA with 20 and 40 wt % PBAT are all higher than that of neat PLA. On the contrary, above 142°C, the crystal-

lization growth rates of PLA in the blends are lower than that of neat PLA. The increase or decrease of the growth rates of PLA in the immiscible blends may be related to the following two facts. First, the addition of low T_g component PBAT decreases the T_g of PLA, resulting in the increase of the chain mobility of PLA molecules. Second, the decrease of the degree of supercooling, i.e., the difference between the equilibrium melting point, T_m^0 , and the crystallization temperature, T_c , may decrease the thermodynamic driving force required for the growth of PLA spherulites. It is strange that blended PLA with 60

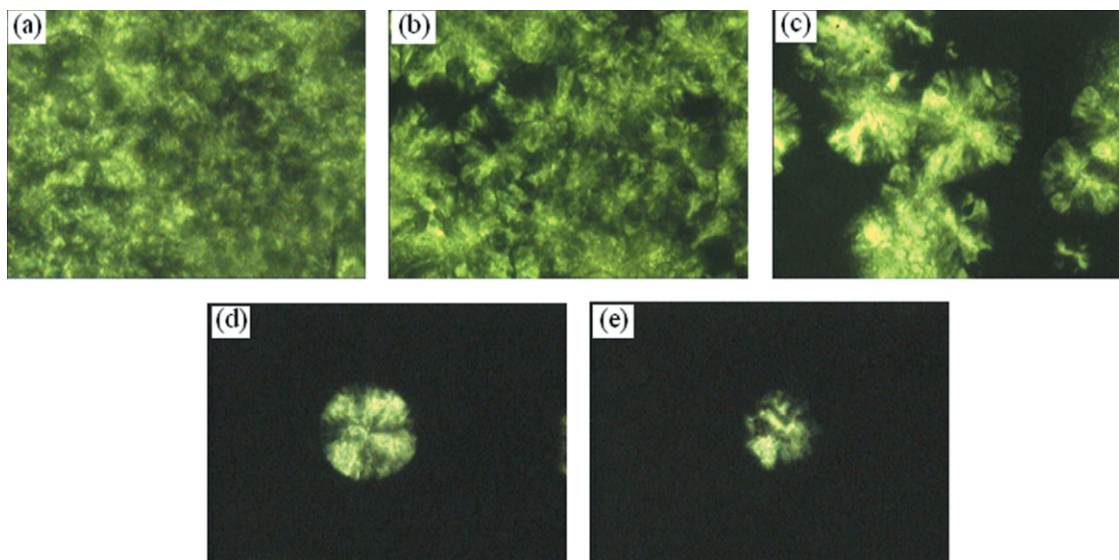


Figure 7 Polarizing optical micrographs of PLA/PBAT (weight ratio: 60/40) crystallized isothermally for 12 min. (a) 123°C; (b) 128°C; (c) 132°C; (d) 137°C, and (e) 142°C. [Color figure can be viewed in the online issue, which is available at www.interscience.wiley.com.]

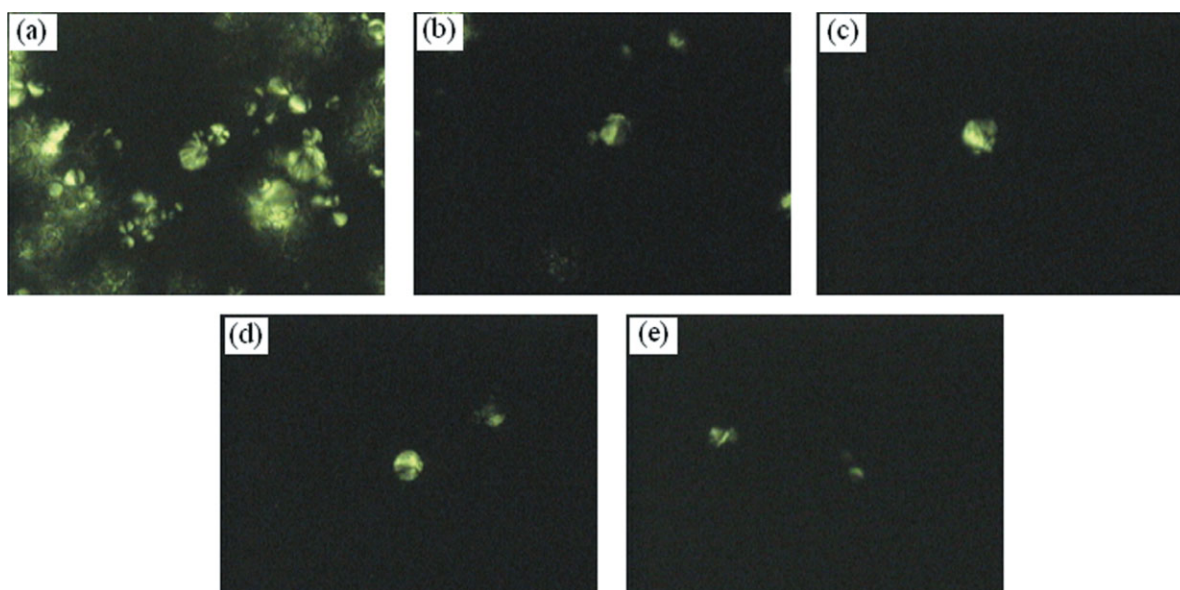


Figure 8 Polarizing optical micrographs of PLA/PBAT (weight ratio: 40/60) crystallized isothermally for 12 min. (a) 123°C; (b) 128°C; (c) 132°C; (d) 137°C, and (e) 142°C. [Color figure can be viewed in the online issue, which is available at www.interscience.wiley.com.]

wt % PBAT has higher equilibrium melting point than those of neat PLA and its blends with 20 and 40 wt % PBAT, but its crystal growth rate is very slow and lower than those of neat PLA and above-mentioned two blends at the temperature range of 123–142°C (not shown in Fig. 9). As previously discussed, it may be related to the values of the energy barriers that need to be overcome to reject and/or deform the noncrystallizable PBAT, which decreases the spherulitic growth rate of PLA in PBAT-rich blends.

DSC analysis

Figure 10 shows the DSC traces of neat PLA, PBAT and their blends at a heating rate of 10°C/min. Table I

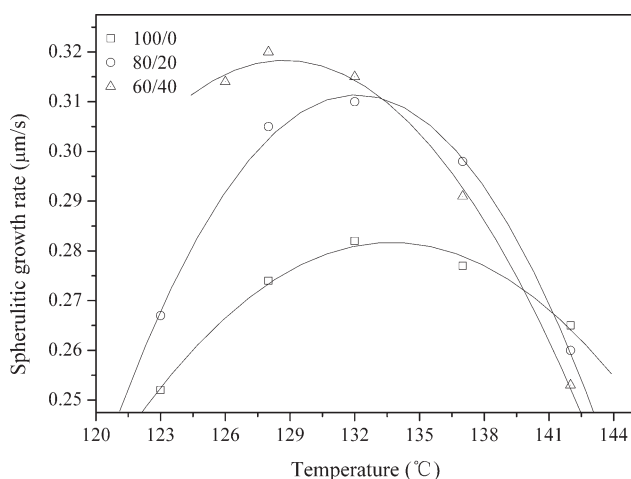


Figure 9 Temperature and component dependence of spherulitic growth rate of PLA and its blends.

shows that the glass transition temperature (T_g) of neat and blended PLA, as well as cold crystallization and melting temperatures (T_{cc} , T_{m1} and T_{m2}). As shown in Table I, neat PLA shows a T_g at 60.7°C, T_g s of PLA in the blends are all lower than that of neat PLA. The amplitude of T_g depression lies between 1.5 and 3.8°C with increasing PBAT content from 20 to 60 wt %. It may be that T_g of PBAT is lower than that of PLA, and the addition of PBAT enhanced the chain mobility of PLA molecules in the blends.

As shown in Figure 10, for neat and blended PLA, neat PLA does not distinctly display a cold crystallization peak, yet cold crystallization peaks are observed in blended PLA at the range of 100.0–104.5°C. The incorporation of PBAT increases cold crystallization temperature and narrows the peak

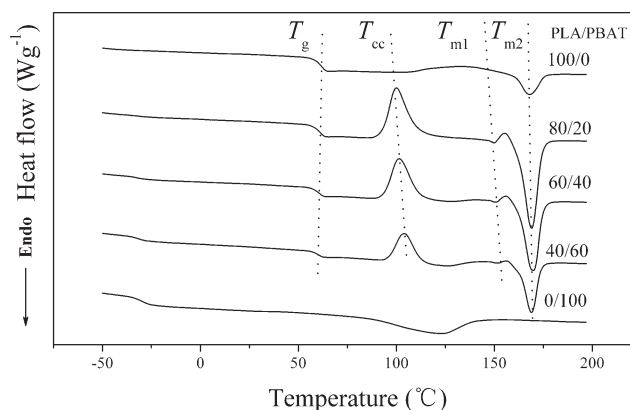


Figure 10 DSC traces of neat PLA and PBAT and their blends.

TABLE I
Result from the Thermal Analysis of PLA, PBAT, and their Blends

PLA/PBAT blends (weight ratios)	ΔH_f (J g ⁻¹)	ΔH_{cc} (J g ⁻¹)	$T_{g,PLA}$ (°C)	T_{cc} (°C)	T_{m_1} (°C)	T_{m_2} (°C)	x_c (%)	x_{cc} (%)
100/0	12.8	–	60.7	–	–	167.4	13.8	–
80/20	33.5	24.4	59.2	100.0	149.4	168.9	45.0	32.8
60/40	26.7	19.1	58.4	101.7	150.1	169.3	47.8	34.2
40/60	16.1	12.2	56.9	104.5	152.3	168.9	43.3	32.8
0/100	21.0	–	–	–	–	121.7	18.4 ^a	–

^a The degree of crystallinity (x_c) of PBAT is estimated from $\Delta H_f/\Delta H_f^0 \times 100\%$, where ΔH_f is the heat of fusion, ΔH_f^0 is the theoretical enthalpy of 114 J g⁻¹ for fully crystalline PBAT.²⁶

width, indicating an enhanced crystalline ability of PLA. The difference between the values of the heat of fusion (ΔH_f and ΔH_{cc}) in crystallization and cold crystallization for each blends (Table I) indicates that PLA in the blends is primarily crystalline. Moreover, the difference decreases with increasing PBAT content, indicating that the degree of crystallinity decreases with the increase of PBAT content when blends are rapidly cooled after the first heating. This can be associated to two different phenomena. The first one is the increased chain mobility at low temperature associated with the larger T_g depression. This T_g reduction enables crystallization to start at an earlier temperature upon heating, for three blends, the amplitude of T_g depression lies between 0.8–2.4°C as shown in Table I. The second phenomenon is the reduced crystallization induction period because of the presence of crystalline nuclei already formed during the cooling process. Even though these nuclei may represent a small crystalline fraction in absolute term, they will increase the crystallization rate upon the second heating, because the crystalline structure is already more densely nucleated than when the polymer are being cooled from the melt. Thus the combination of reduced T_g and less crystalline nuclei results in cold crystallization peaks that are shifted to a higher temperature as the PBAT content is increased.

Interestingly, melting endotherms of PLA in the blends show two distinct peaks compared to neat PLA as shown in Figure 10. The double melting peaks of PLA, which have been attributed to lamellar reorganization,^{27,28} become more pronounced at lower PBAT content. As a result of lamellar rearrangement during crystallization of PLA: a ‘shoulder’ or low-temperature peak is formed on the melting endotherm of the original crystallites. Besides, the different crystalline structures that can exist in PLA have been described by Cartier et al.²⁹ The higher temperature melting point of neat PLA is 167.4°C. There are, however, some differences when the PLA in the blends with different PBAT contents are considered. At first, the melting points of blends increased by 0.4°C when PBAT contents in the

blends change from 20 to 40 wt %, then decreased by 0.4°C when PBAT contents in the blends change from 40 to 60 wt %. Table 1 shows that the neat PLA is very weakly crystallized because it presents a melting endotherm at 167.4°C with an enthalpy of 12.8 J g⁻¹ in comparison to thermodynamical melting enthalpy of 93 J g⁻¹ for fully crystalline PLA.¹⁹ The degree of crystallinity was calculated based on the following equation:

$$x_c = \frac{\Delta H_f}{w_{PLA} \times \Delta H_f^0} \times 100\% \quad (1)$$

where ΔH_f is the heat of fusion, ΔH_f^0 is the heat of fusion for 100% crystalline PLA, and w_{PLA} is weight fraction of PLA in the blends. According to Table I, the degrees of crystallinity of three blends with various PBAT contents are all higher than that of neat PLA. It should be noted that the degrees of crystallinity of blends obtained by eq. (1) are from two parts: one is from the first rapid cooling from the melt and the degree of crystallinity are decreased with increasing PBAT content. The other is the second heating after the rapid cooling, i.e., cold crystallinity, the degrees of cold crystallinity of three blends initially increase, and then decrease with increasing PBAT content. Final degrees of crystallinity of three blends are equal to or lower than that of neat PLA if the degree of cold crystallinity is not taken into account as listed in Table I. The first phenomenon can be explained that on one hand, the incorporation of a small amount of PBAT increases the growth rate of spherulites and the nucleation rate, on the other hand, decreases the number of crystal nuclei, which offsets the previous two effects and results in the degree of crystallinity that is decreased as the PBAT content is increased upon rapid cooling. The incorporation of a large amount of PBAT increases the nucleation rate, but decreases the number of crystal nuclei and the growth rate of spherulites, which results in the degree of crystallinity which is decreased. The second phenomenon can be explained that crystalline nuclei already formed during the first cooling process, the number of

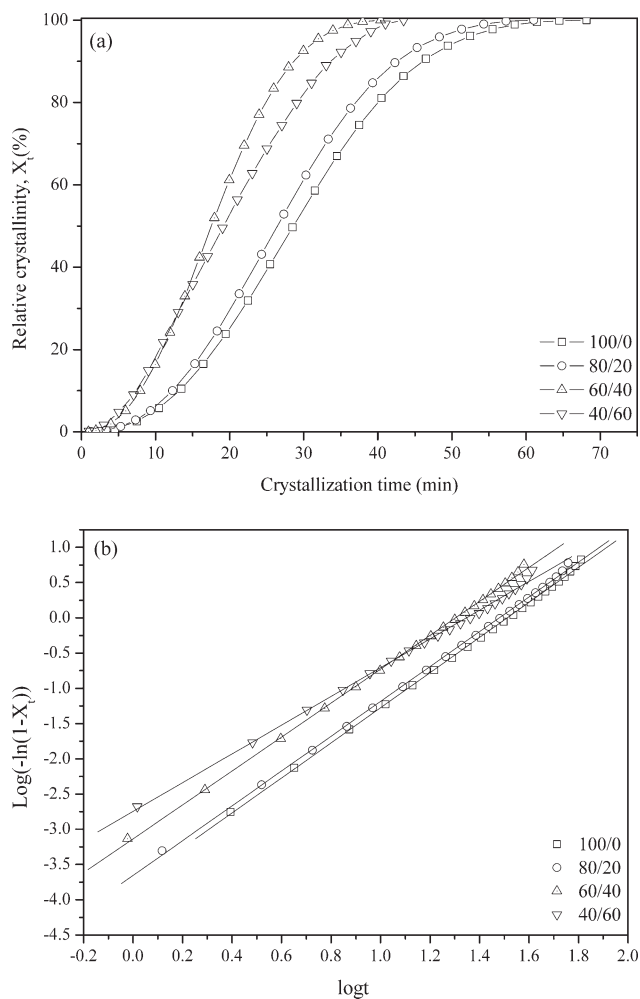


Figure 11 (a) Plots of relative crystallinity as a function of crystallization time for neat PLA and its blends at 128°C, and (b) Avrami plots for neat PLA and its blends at 128°C.

crystalline nuclei decreases with increasing PBAT content and these nuclei will increase the crystallization rate upon the second heating. In addition, the PBAT increases the chain mobility of PLA molecules at the low temperature and decreases T_g of PLA, which favors the crystallization growth of PLA in the blends. The combination of three effects results in the degree of crystallinity that is initially increased and then decreased when PBAT content is increased from 20 to 40, and then 60 wt %.

Crystallization kinetic

The process of the isothermal crystallization of neat PLA and its blends was investigated at crystallization temperature of 128°C. The plots of relative crystallinity X_t versus the crystallization time t are shown in Figure 11(a) for the isothermal crystallization at 128°C of neat and blended PLA. It was found that the crystallization time for PLA at 128°C short-

ened in the blends compared to neat PLA. The well-known Avrami equation was often used to analyze the isothermal crystallization kinetics^{30–32}: it assumes that the relative degree of crystallinity develops with crystallization time t as

$$1 - X_t = \exp(-kt^n) \quad (2)$$

where X_t is the relative degree of crystallinity at time t ; the exponent n is a mechanism constant with a value depending on the type of nucleation and the growth dimension, and the parameter k is a growth rate constant involving both nucleation and the growth rate parameters.³³ The plot of $\text{log}(-\ln(1-X_t))$ versus $\text{log} t$ according to eq. (2) was shown in Figure 11(b). The crystallization process is usually treated as two stages: the primary crystallization stage and the secondary crystallization stage. Carefully observed Figure 11(b), one can see that all curves are divided into two sections—the primary crystallization stage and the secondary crystallization stage, which become more obvious as the addition of PBAT. This deviation indicates that the existence of the secondary crystallization of the blends at longer crystallization time. It is generally believed that the secondary crystallization is caused by the spherulite impingement in the later stage of crystallization process.^{34–36} By comparing four curves measured at 128°C, as shown in Figure 11(b), the occurring time of secondary crystallization of neat and blended PLA are different. Generally speaking, secondary crystallization of PLA in the blends is much shorter than that of the neat PLA. This fact indicates that without the incorporation of PBAT, the nuclei in the neat PLA grow slowly into spherulites before they impinge against each other. PBAT causes crystallization of PLA completed earlier because PBAT melt in the blends accelerates formation of PLA crystal nuclei and then impinge against each other.

The Avrami parameters n and k are obtained from the plots of $\text{log}(-\ln(1-X_t))$ versus $\text{log} t$ as shown in Figure 11(b). The Avrami exponent n and crystallization rate constants k of neat and blended PLA are shown in Table II. The average values of n are around 2.3. It is an average value of various

TABLE II
Crystallization Kinetic Parameters of PLA and its blends at 128°C

PLA/PBAT	n	k (min ⁻ⁿ)
100/0	2.5	5.5×10^{-5}
80/20	2.5	7.2×10^{-5}
60/40	2.4	2.4×10^{-4}
40/60	2.0	7.0×10^{-4}

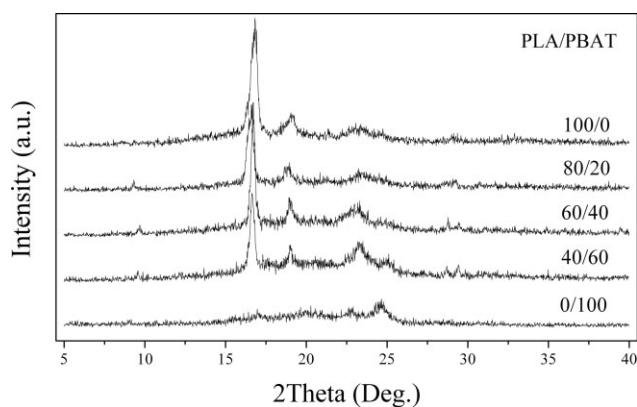


Figure 12 WAXD patterns of neat PLA and PBAT and their blends.

nucleation types and the growth dimensions occurred simultaneously in a crystallization process. For neat PLA, its nucleation type should predominantly be homogenous nucleating and its growth dimensions should predominantly be a two-dimensional growth. For the PLA/PBAT blends, its nucleation type should mainly be heterogeneous nucleating and its growth dimension should mostly be two-dimensional space extension. The values of n are close to 2 for the isothermal crystallization of both neat and blended PLA may indicate that the crystallization mechanism of PLA is almost not affected in the presence of PBAT melt in PLA/PBAT blends. On the other hand, the values of k in the blends are higher than that of neat PLA, indicating that blending with PBAT enhanced the crystallization rate of PLA, which is agreement with the result in the Figure 9. For both neat and blended PLA with various 20 and 40 wt % PBAT, two possible reasons are proposed to explain the speed-up of the crystallization rate of PLA. One is the presence of the PBAT accelerated the nucleation of the PLA in the blends. In other words, the presence of PBAT has a positive effect on the primary nucleation of PLA. But the number of nuclei of PLA may decrease with the addition of PBAT in the blends because of the diluting effect of PBAT. The other is the increase of crystallization rate of PLA in the blends might be attributed to the increase of nucleation rate of PLA in the blends. PLA and PBAT are immiscible,¹⁴ and the interface of the phase separated domains may provide favorable nucleation sites for crystallization of PLA. Therefore, the crystal rate of PLA was enhanced by lowering the nucleation barrier in the blends than that of neat PLA. Similar results were also found in PLA/PCL and PLA/PES blends, and it was reported that the crystallization rate of PLA increased also with increasing PCL and PES content in the blends.^{4,18} In addition, T_g depression has a positive effect on crystallization rate of PLA because

of the incorporation of PBAT. In the case of blended PLA with 60 wt % PBAT, even though the spherulitic growth rate of PLA is lower than those of blended PLA with 20 and 40 wt % PBAT, yet the crystallization rate of PLA is still higher than those of two blends with 20 and 40 wt % PBAT. It should be emphasized that overall crystallization rates are not as easy to interpret as spherulitic radial growth because of the combination of nucleation and growth phenomena. It may be that blend with 60 wt % PBAT has high nucleation rate, relative low growth rate, but the form plays a dominant role in the total crystallization rate.

XRD analysis

The diffraction traces of neat PLA, PBAT and their blends films at room temperature are shown in Figure 12. Neat PLA presented two strong diffraction peaks at around 16.7° and 18.8° corresponding to (200)/(110) and (203) planes, respectively.³⁷ Four diffraction peaks of the PBAT crystal structure are observed at angle 2θ 17.4° , 20.8° , 22.8° , and 24.4° , respectively. For PLA/PBAT blends, they involved all the diffraction peaks corresponding to both neat PLA and PBAT, and the intensity of the diffraction peaks of each component decreased with increasing the other component content in the blends. Such results indicate that PLA blending with PBAT don't modify the crystal structure in the blends. But the decrease of intensity of the diffraction peaks indicates that the degree of crystallinity of PLA decreases. It is related to the process by which samples are prepared because they are quenched from the melt and obtained directly and the degrees of crystallinity of PLA in the blends are almost decreased with increasing PBAT content. Similarly, PLA blending with PBAT also decreased the degrees of crystallinity of PBAT, leading to the decrease of intensity of diffraction peaks corresponding to crystal structure of PBAT.

CONCLUSIONS

Isothermal crystallization kinetic and morphology of biodegradable crystalline/semicrystalline PLA/PBAT blends were investigated with DSC, POM and WAXD in detail in this work. The overall isothermal crystallization kinetic of neat and blended PLA was studied with DSC and analyzed by the Avrami equation. The Avrami exponent n was almost unchanged despite the crystallization temperature and the addition of amorphous PBAT, indicating that blending with PBAT almost did not change the crystallization mechanism of PLA at the crystallization temperature of 128°C . However, the crystallization rate increased with the increase PBAT content,

except for PLA blend with 60 wt % PBAT. The variation of the overall crystallization rate was mainly attributed to two factors, including the variation of T_m^0 and the decrease of T_g . The spherulitic morphology and growth were observed with hot stage POM in a wide crystallization temperature range of 123–142°C. The spherulitic morphology of PLA was influenced apparently by crystallization temperature and the blending with PBAT. The crystal structure of PLA was not modified by the blending, and the crystal structure almost remains unchangeable from the WAXD measurement.

References

- Zhang, J.; Duan, Y.; Sato, H.; Tsuji, H.; Noda, I.; Yan, S. Y.; Ozaki, Y. *Macromolecules* 2005, 38, 8012.
- Gazzano, M.; Focarete, M. L.; Riekkel, C.; Scandola, M. *Biomacromolecules* 2004, 5, 553.
- Hoogsteen, W.; Postema, A. R.; Pennings, A. J.; ten Brinke, G.; Zugenmaier, P. *Macromolecules* 1990, 23, 634.
- Liu, J. M.; Qiu, Z. B.; Yang, W. T. *Polymer* 2007, 48, 4196.
- Blümm, E.; Owen, A. J.; *Polymer* 1995, 36, 4077.
- Focarete, M. L.; Ceccorulli, G.; Scandola, M.; Kowalczyk, M. *Macromolecules* 1998, 31, 8485.
- Shirahase, T.; Komatsu, Y.; Tominaga, Y.; Asai, S.; Sumita, M. *Polymer* 2006, 47, 4839.
- Meaurio, E.; Zuza, E.; Sarasua, J. R. *Macromolecules* 2005, 38, 1207.
- Ogata, N.; Jimenez, T. *J Polym Sci Part B: Polym Phys* 1997, 35, 389.
- Park, E. U.; Kim, H. K.; Shim, J. H.; Kim, H. S.; Jang, L. W.; Yoon, J. S. *J Appl Polym Sci* 2004, 92, 3508.
- Ferreira, B. M. P.; Zavaglia, C. A. C.; Duek, E. A. R. *J Appl Polym Sci* 2002, 86, 2898.
- Tsuji, H.; Muramatsu, H. *J Appl Polym Sci* 2001, 81, 2151.
- Pezzin, A. P. T.; Alberda van Ekenstein, G. O. R.; Zavaglia, C. A. C.; Ten Brinke, G.; Duek, E. A. R. *J Appl Polym Sci* 2003, 88, 2744.
- Jiang, L.; Wolcott, M. P.; Zhang, J. *Biomacromolecules* 2006, 7, 199.
- Zhang, N. W.; Wang, Q. F.; Ren, J.; Wang, L. *J Mater Sci* 2009, 44, 250.
- Shi, X. Q.; Ito, H.; Kikutani, T. *Polymer* 2005, 46, 11442.
- Chivrac, F. R.; Kadlecová, Z.; Pollet, E.; Avérous, L. *J Polym Environ* 2006, 14, 393.
- Dell'Erba, R.; Groeninckx, G.; Maglio, M.; Malinconico, M.; Migliozi, A. *Polymer* 2001, 42, 7831.
- Fisher, E. W.; Sterzel, H. J.; Wegner, G.; Kollid, Z. Z. *Polymer* 1973, 251, 980.
- Hoffman, J. D.; Weeks, J. J. *J Res Natl Bur Std A* 1962, 66A, 13.
- Tsuji, H.; Ikada, Y. *Polymer* 1995, 36, 2709.
- Silvestre, C.; Cimmino, S.; Di Pace, E.; Martuscelli, E.; Monaco, M.; Buzarovska, A.; Koseva, S. *Polym Network Blends* 1996, 6, 73.
- Avella, M.; Martuscelli, E.; Orsello, G.; Raimo, M.; Pascucci, B. *Polymer* 1997, 38, 6135.
- Yokoyama, Y.; Ricco, T. *J Appl Polym Sci* 1997, 66, 1007.
- Martuscelli, E. *Polym Eng Sci* 1984, 24, 563.
- Herrera, R.; Franco, L.; Rodriguez-Galan, A.; Puiggali, J. *J Polym Sci Part A: Polym Chem* 2002, 40, 4141.
- Martin, O.; Avérous, L. *Polymer* 2001, 42, 6209.
- Nijenhuis, A. J.; Colstee, E.; Grijpma, D. W.; Pennings, A. *J Polymer* 1996, 37, 5849.
- Cartier, L.; Okihara, T.; Ikada, Y.; Tsuji, H.; Puiggali, J.; Lotz, B. *Polymer* 2000, 41, 8909.
- Avrami, M. *J Chem Phys* 1941, 9, 177.
- Tobin, M. C. *J Polym Sci Part B: Polym Phys* 1974, 12, 399.
- Tobin, M. C. *J Polym Sci Part B: Polym Phys* 1976, 14, 2253.
- Avrami, M. *J Chem Phys* 1939, 7, 1193.
- Wunderlich, B. *Macromolecular Physics*. Vol. 2; Academic Press: New York, 1977.
- Liu, J. P.; Mo, Z. S. *China Polym Bull* 1991, 4, 199.
- Liu, T.; Mo, Z.; Wang, S.; Zhang, H. *Polym Eng Sci* 1997, 3, 568.
- Ueda, A. S.; Chatani, Y.; Tadokoro, H. *Polymer J* 1971, 2, 387.